



Preparing and Characterizing Some New Compounds of Schiff Bases Loaded on Polymers Dissolved in Water, Studying Some of their Physical Properties, And Evaluating their Biological Effectiveness

1. Ammar Ibrahim Mardan Al-Obaidi
2. Nabil Jamal Ayed Al-assly

Received 2nd Aug 2023,
Accepted 19th Aug 2023,
Online 12th Sep 2023

^{1,2} Department of Chemistry - College of Education for Pure Sciences - Tikrit University, Tikrit-Iraq

Abstract: This research included the preparation of Schiff bases [KB7-KB11] from the reaction of 2-pyrrolidone with amines, and the compounds were identified using FT-IR spectroscopy techniques, ¹H-NMR using DMSO-d₆ as a solvent, SEM, and thermal analysis in addition to the melting point. This work also included studying the biological activity of some compounds prepared on two types of Gram-positive and Gram-negative bacteria, these include (Staphylococcus aureus, Klebsiella pneumonia) and Acar Mueller-Hinton culture medium. (Molar Hunting Agar) Aqueous solutions were prepared at concentrations (0.01, 0.001, 0.0001) mg/ml also using dimethyl sulfoxide (DMSO) as a solvent. The susceptibility test of the bacterial isolates used in the study was carried out by diffusion method, and the antibiotic Ampicillin was used as a control sample. The electrical conductivity and synthetic stability of some of the prepared compounds were also studied.

Key words: Schiff bases, 2-pyrrolidone, Staphylococcus aureus, Klebsiella pneumoniae.

1. Introduction

They are compounds that contain the azomethine functional group (-HC=N-) in their chemical structure. They are mainly distinguished by their yellow color. They have the general formula (R₁R₂C=NR₃). These compounds are named after the scientist Hugo Schiff, who attended them for the first time. , , where these compounds were prepared from a simple condensation of aldehydes or ketones with aromatic or aliphatic primary amines (1).

Schiff bases are named according to the nature of the groups (R₁, R₂, R₃), so they are called relative to the amine, aldehyde, or ketone derived from them, where Schiff bases derived from the condensation of aliphatic or aromatic aldehydes with aliphatic or aromatic primary amines are called diamines (2), either when Aliphatic or aromatic ketones are condensed with aliphatic or aromatic

primary amines as ketimines (3), and when aldehydes and aliphatic or aromatic ketones are condensed with aniline or one of its enyl derivatives (4), Schiff bases derived from the condensation of an aldehyde or ketone with the hydrazides of suitable acids are called hydrazones (5).), and when the aldehyde, aliphatic ketone, or aromatic hydroxylamine is condensed with oximes (6). Schiff bases also have some common names such as imines, benzanylates, and azomethines (7). In general, it is preferable for these compounds to contain an aryl group on the carbon or nitrogen atom to increase To ensure its stability and to protect it from disintegration (8).

2- Pyrrolidone, which is one of the pyrrolidine derivatives, and is known as 2-pyrrolidinone or butyrolactam. It is an organic compound consisting of five lactam molecules (9). It is a colorless liquid at a temperature higher than 25oC. Its molecular weight is 297 K (10). It is miscible with water, ether, chloroform, and benzene (11). 2-pyrrolidone is the simplest pyrrolidone derivative. It is prepared by hydrogenation of succinamide to produce 2-pyrrolidone, and after hydrogenating it, pyrrolidone can be produced ((12.

2- Pyrrolidone is used in the production of industrial resins and fibers (13), and is used in the formulation of insecticides (14). It is also used in the manufacture of printing inks and in the manufacture of polyvinylpyrrolidone (15). It is also used in industrial settings as a non-corrosive polar solvent for a variety of purposes. Among the applications (16), it is also used in the manufacture of many medications, the most important of which are cotinine, doxapram, piracetam, povidone, and ethosuximide (18,17)

2. Experimental

2.1. Material: All chemicals were used through this work purchased from Fluka, Aldrich, BDH Companies.

2.2. Devices used: Melting points were recorded using a measuring device melting point type: Automatic melting point\SMP40 and were uncorrected. Thin layer chromatography (TLC) was carried out using sheet polygram silica- gel as stationary phase, the spots were enhanced using Iodine. Infrared spectra were recorded using FT-IR-600 Fourier- Transform infrared Spectrophotometer by KBr disc and with a scale of (400-4000) cm^{-1} . The nuclear magnetic resonance (^1H , ^{13}C -NMR) spectra were measured for the compounds prepared in the laboratories of Sannati Sharif University - Iran, using MS5973 Agilent Technology, Germany Bruker 500 MHz, at 500 MHz, and using (DMSO- d^6) as a solvent

2.3. Preparing the rules of Shaf:

2.3.1. Preparation of the compound [KB7] (19)

I dissolved 0.01 mole of substituted pyrrolidone in 20 ml of methanol in a 100 ml round flask and with continuous stirring, (0.01 mole) of aspartate dissolved in the same solvent was added gradually with stirring for a full hour and no precipitation occurred. The mixture was heated for three hours at a temperature of (120oC), then cooled in an ice bath until a precipitate formed, filtered and recrystallized using methanol. The compounds [KB8, KB9, KB10] were prepared in the same way.

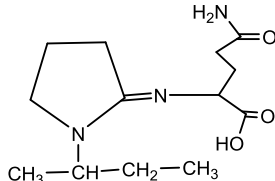
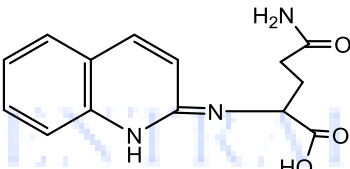
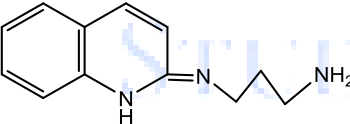
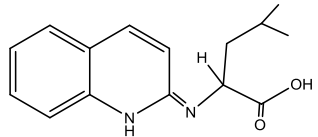
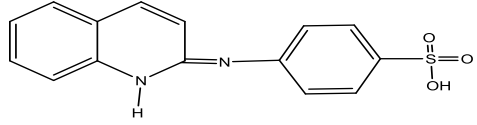
2.3.2. Preparation of the compound [KB11] (20)

Mixing (0.01 mole) of pyrrolidone with (0.01 mole) of leucine in a ceramic mortar, where it was ground well for an hour. A portion of the prepared material was taken and heated for (5-7) minutes at a temperature of 150oC, where it was melted. We notice its color changing from white to The yellow color and strong gaseous release are evidence of the formation of the product. Then I left the material and it solidified.

Table 1: Some physical properties and product percentages for monomers (KB7-KB11)

Comp. No.	طريقة التحضير	Molecular Formula	Color	M.P °C	Yield %
KB7	الطريقة 1	C ₁₃ H ₂₃ N ₃ O ₃	White	Gum	70%
KB8	الطريقة 2	C ₁₄ H ₁₅ N ₃ O ₃	White	200-202	74%
KB9	الطريقة 1	C ₁₂ H ₁₅ N ₃	Yellow	Gum	68%
KB10	الطريقة 2	C ₁₅ H ₁₈ N ₂ O ₂	Yellow	220-222	65%
KB11	الطريقة 2	C ₁₆ H ₁₆ N ₂ O ₃ S	Yellow	190-192	77%

Table (2) Prepared compounds

KB7	 <p>(Z)-5-amino-2-((1-(<i>sec</i>-butyl)pyrrolidin-2-ylidene)amino)-5-oxopentanoic acid</p>
KB8	 <p>5-amino-5-oxo-2-(quinolin-2(1<i>H</i>)-ylideneamino)pentanoic acid</p>
KB9	 <p>(Z)-3-(quinolin-2(1<i>H</i>)-ylideneamino)propan-1-amine</p>
KB10	 <p>(<i>E</i>)-4-methyl-2-(quinolin-2(1<i>H</i>)-ylideneamino)pentanoic acid</p>
KB11	 <p>4-(quinolin-2(1<i>H</i>)-ylideneamino)benzenesulfonic acid</p>

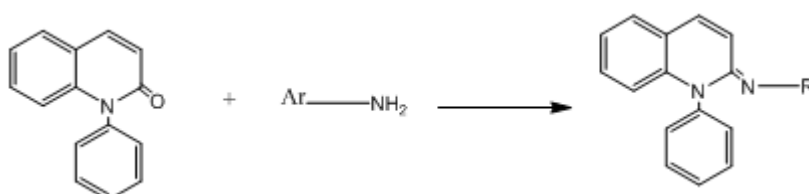
2.4. Study of biological activity (21, 22):

This study was used on two types of pathogenic bacteria, Gram-positive and Gram-negative: *Staphylococcus aureus* and *Klebsiella pneumonia*, which are essential in the medical field due to their resistance to antibiotics. These bacteria were taken from the laboratories of the College of Education for Pure Sciences, Department of Biosciences, and Mueller-Hinton-Agar culture medium was used. Molar Huntin Agar) is used to measure the biological activity of antibiotics and chemicals for medical uses and is used to measure and determine the minimum inhibitory limit (MIC). Aqueous solutions of the two compounds [KB7, KB11] were also prepared. At concentrations (0.01, 0.001, 0.0001 mg/ml)

and using the solvent dimethyl sulfoxide (DMSO), susceptibility testing was performed for the bacterial isolates used in the study by the diffusion method in the nutrient medium of Mueller-Hinton agar, which is a transparent nutrient medium with a dark yellow color. D in testing the sensitivity of microorganisms to antibiotics because it contains an animal infusion extracted from casein and starch

3. Results and discussion:

Schiff bases (KB7-KB11) were prepared by reacting pyrrolidone with amino acids in the presence of a suitable solvent, as shown in the following equation.



Observed from the ultraviolet (U.V.) spectrum of the derivatives of the prepared Schiff bases, we notice the appearance of an absorption band with greater intensity and shorter wavelength attributed to the electronic transitions $\pi \rightarrow \pi^*$ and caused by bonds ($C=C, C=O, C=N$), which appears pathochromically displaced in the derivatives of Schiff bases prepared within the range (230-280) nm. A band with a longer wavelength and lower intensity also appears, as this is attributed to $n \rightarrow \pi$ electronic transitions. *It is caused by the unshared electron pairs present on the oxygen and nitrogen atoms, and these bands appear pathochromically displaced in the prepared compounds due to the presence of oxo groups and succession within the range of (320-360) nm (23).

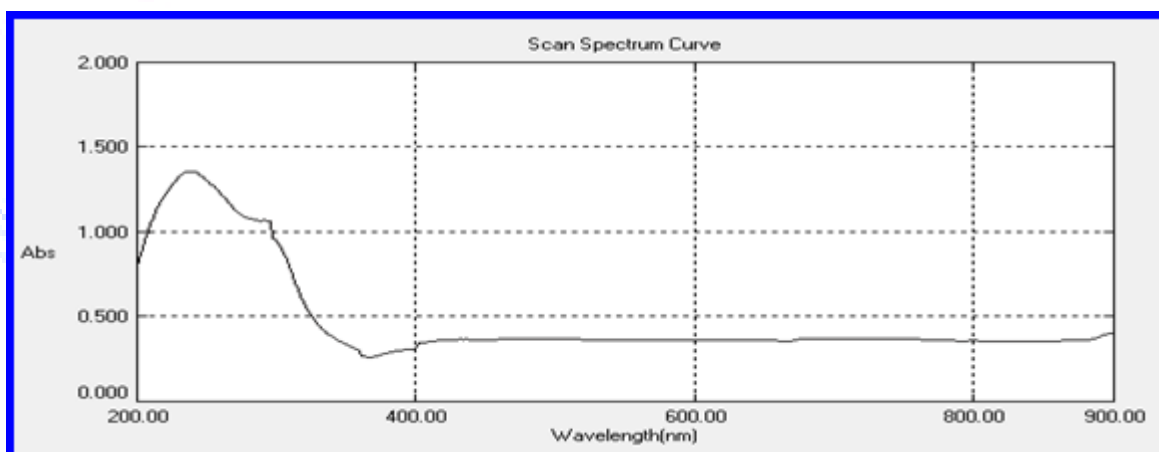
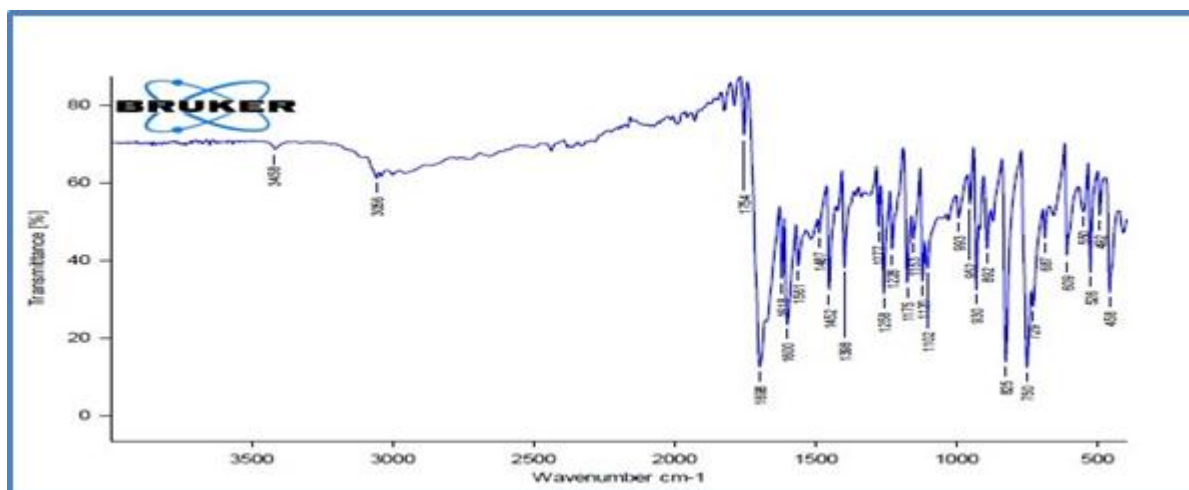


Figure (1): represents the ultraviolet spectrum of the compound [K8]

The infrared spectrum of the prepared Schiff bases [KB8] Figure (2) showed absorption bands within the range (1581cm^{-1}) due to the stretching of the bond ($C=N$), with two bands appearing at the range (3056cm^{-1}) and one band at the range ($1618\text{-}1600\text{cm}^{-1}$). 1) It belongs to the olefinic group ($C=C$), as well as a band at the range (1487cm^{-1}) that belongs to the stretching of the aromatic ($C=C$), in addition to the absorption band that appeared at the range (1754cm^{-1}) that belongs to the stretching of the carbonyl group ($C=O$).) The ring and the absorption band that appeared at the range (1698 cm^{-1}) are due to the stretching of the carboxyl carbonyl ($C=O$) group, with the disappearance of the stretching band that belongs to the amine group of the pyrrolidone (24).



The infrared spectrum of the compound [KB11] in Figure (3) showed a band in the range (1580 cm^{-1}) dating back to stretching the (C=N) group, and a band within the range (3415 cm^{-1}) dating back to stretching the (OH) group, with two bands appearing at The range (1753-1701 cm^{-1}) is due to the stretching of the carbonyl group (C=O), as well as a band in the range (1589 cm^{-1}) that is due to the olefinic (C=C), in addition to an absorption band in the range (2914 cm^{-1}) that is due to the stretching of the sphincter (-C-H) aliphatic with the disappearance of the stretch band belonging to the amine group (24).

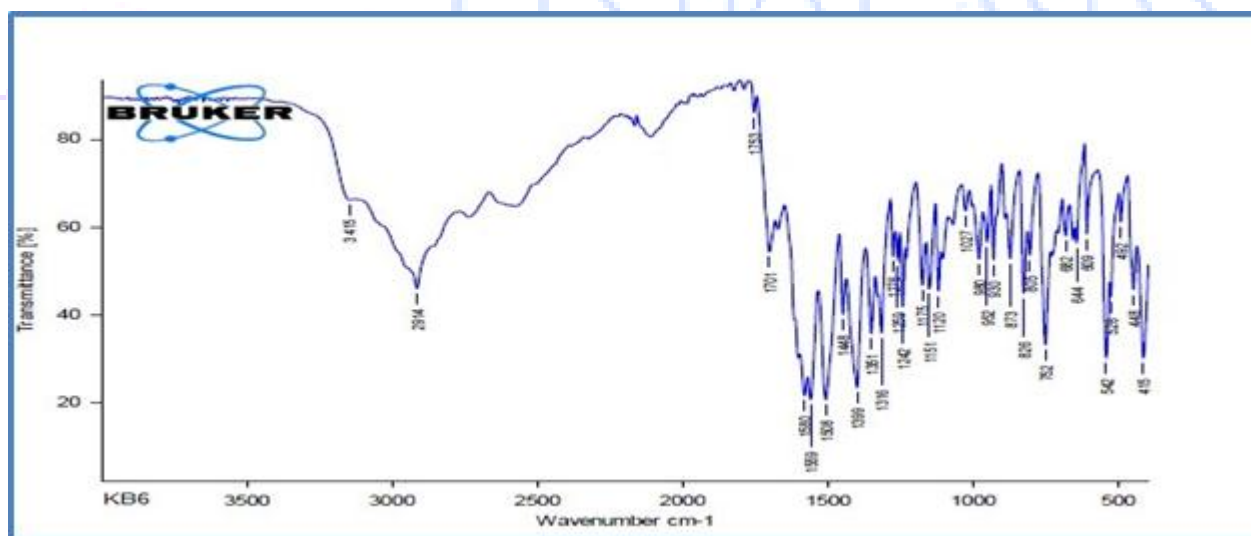


Figure (3): represents the infrared spectrum of the compound [KB11]

Table (3): Infrared spectrum absorption results (cm^{-1}) for derivatives of Schiff bases (NKB8-KB11)

Comp. No.	IR , (KBr), cm^{-1}					
	ν (CH) olefenic aromatic aliphatic	ν C=O amid & carboxyl ν C=N	ν (C=C) olefenic or aromatic	ν C- O	ν C- N	Other
KB7	3186,3062,2950-2999	1723,1689 1589	1514 ,1454	1221	1122	δ (C-H) aromatic 796 ν (OH) 3434

KB8	3203,2835-2991	1754,1698, 1618	1600, 1581,1487	1228	1120	δ (C-H) aromatic 750 ν (OH) 3458
KB9	3066,2975-2851	1723,1698 1568	1568-1415, 1415-1373,	1271	1033	δ (C-H) aromatic 798 ν (NH ₂) 3458
KB10	3286-3128,3087 2987-2887	1711 1691 1587	1575,1452 1424	1228	1121	δ (C-H) aromatic 787 ν (OH) 3324
KB11	2914	1753,1701 1580	1559,1508 1448	1242	1120	δ (C-H) aromatic 752 ν (OH) 3415

¹H proton nuclear magnetic resonance (NMR) spectrum

We note from the NMR spectrum of the proton NMR - ¹H of the compound [KB8] a single signal at the position (12.22) ppm attributed to the hydroxyl proton, and the signal at the position (11.65) ppm attributed to the (NH) proton, and a signal at the position (7.96) ppm is attributed to the proton attached to the heterocyclic ring, and the emergence of multiple signals at (7.07-6-80) ppm due to the protons of the aromatic ring, and the spectrum showed multiple signals at the location (6.34) ppm dating back To a proton attached to the heterocyclic ring at the meta site, and a sign at the position (2.31-2.08) ppm attributed to the protons (CH₂-CH₂) attached to the carbonyl groups, and a signal at the position (1.65) ppm attributed to the proton (CH₂) (25), and as shown in Figure (4).

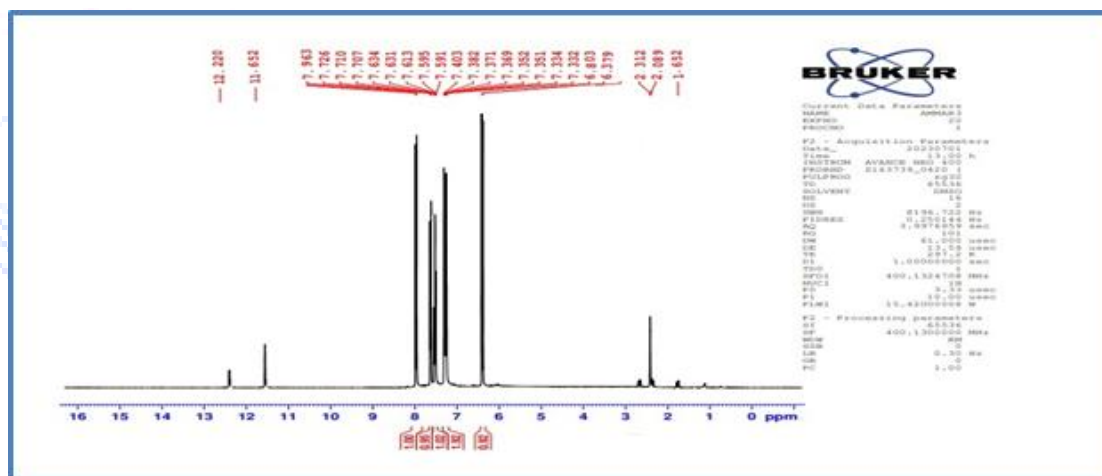


Figure 4: ¹H-NMR spectrum of compound [KB8]

The ¹H proton NMR spectrum of the compound [KB11] showed a single signal at the site (11.68) ppm attributed to the proton attached to the heterogeneous ring, and the spectrum showed a signal at the site (8.58) ppm attributed to the hydroxyl proton, and the appearance of signals Multiple at (7.80-6-72) ppm due to the protons of the aromatic ring, and a signal at the site (6.48) ppm due to a proton attached to the heterocyclic ring at the meta site (25), and as shown in Figure (5).

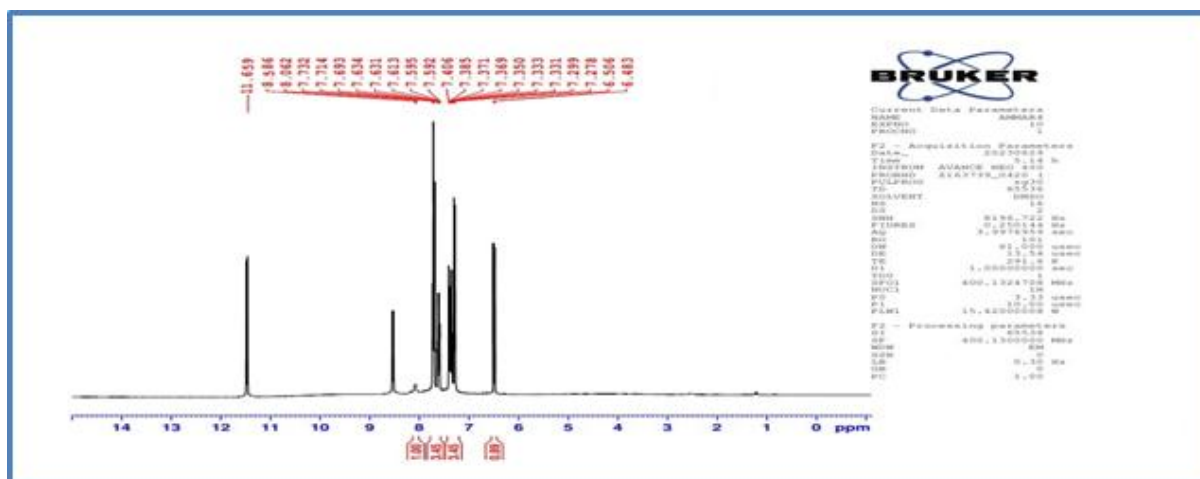


Figure (5): ^1H -NMR spectrum of the compound [KB11]

We note from the ^{13}C -NMR spectrum of the compound [KB8] that a signal appeared at 177 ppm attributed to the carbonyl carbon attached to the (OH) group, and a signal appeared at 173 ppm attributed to the carbonyl carbon attached to the (NH₂) group. The signal at 158 (ppm) belongs to the carbon of the azomethine group, and the signal at 145 (ppm) refers to the carbon of the heterogeneous ring attached to the (NH) group. Multiple signals appeared at (137-113) ppm attributed to the carbons of the aromatic ring and the ring. Heterogeneous, a signal appeared at (66) ppm and belonged to the carbon attached to the carboxyl group, and the signal at (33-30) ppm was attributed to the carbons (CH₂-CH₂) attached to the carbonyl group (26), as shown in Figure (6).

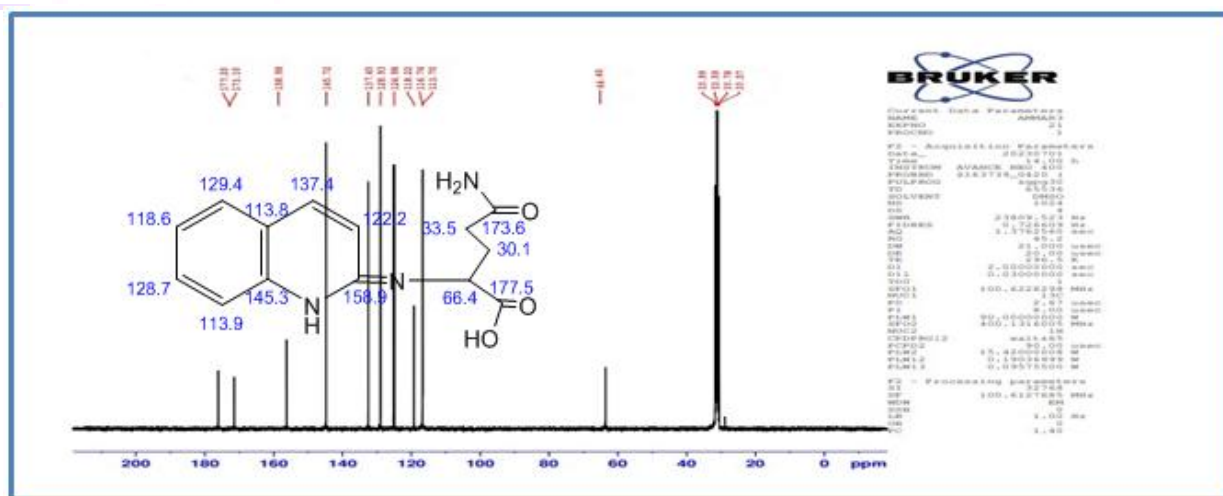


Figure (6): ^{13}C -NMR spectrum of the compound [KB8]

We note from the ^{13}C -NMR nuclear magnetic resonance spectrum of the compound [KB11] a signal at 158 (ppm) due to azomethine carbon, and a signal appeared at 153 (ppm) due to the carbon attached to azomethine nitrogen, and the signal at 144 (ppm) is due to Carbon has the aromatic ring connected to sulfur, and the signal at (137) ppm belongs to the heterocyclic carbon in the Bara site, and multiple signals appeared at (113-128) ppm attributed to the carbons of the aromatic ring and the heterocycle (26), as shown in the figure (7)

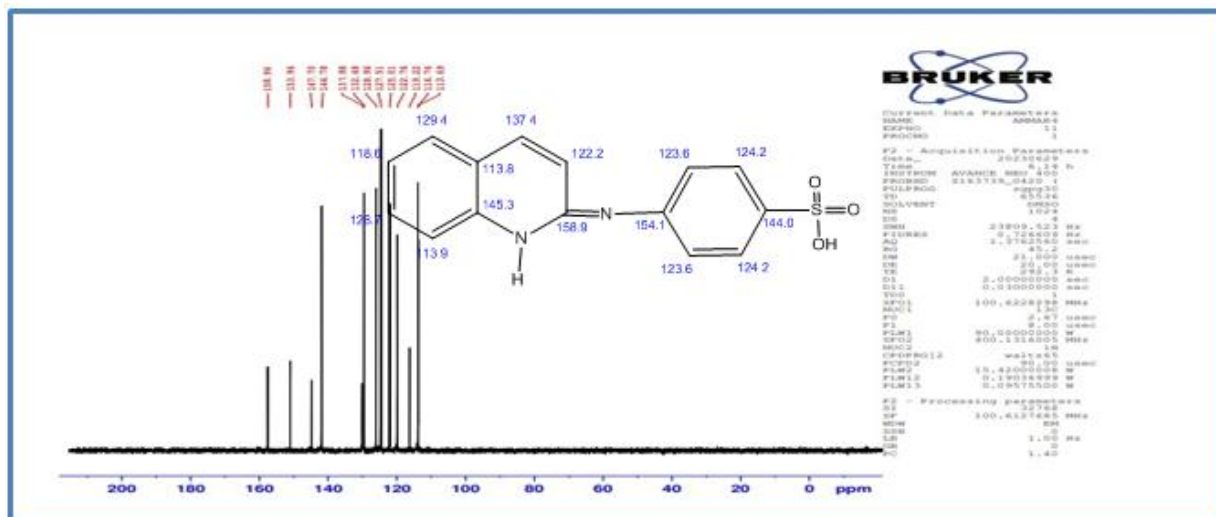


Figure (7): ^{13}C -NMR spectrum of the compound [KB11]

Mass spectrum mass

To prove the structures of the prepared materials, a mass analysis was conducted in order to determine their molecular weight, using the peak of its molecular ion and other peaks of the generated fragments, and the main peak of the molecule after ionization (27). The mass spectrum of the compound showed [KB8 M.Wt = 273] several fissions, as it appeared A peak at $m/z=256$ [$\text{C}_{14}\text{H}_{14}\text{N}_3\text{O}_2$], a second peak at $m/z=229$ [$\text{C}_{13}\text{H}_{15}\text{N}_3\text{O}$], a third peak at $m/z=213$ [$\text{C}_{13}\text{H}_{13}\text{N}_2\text{O}$], the fourth peak appeared at $m/z=186$ [$\text{C}_{12}\text{H}_{14}\text{N}_2$], and the fifth peak at $m/z=158$ [$\text{C}_{10}\text{H}_{10}\text{N}_2$], the seventh peak is at $m/z=144$ [$\text{C}_9\text{H}_8\text{N}_2$], the eighth peak is at $m/z=131$ [$\text{C}_9\text{H}_9\text{N}$], the ninth peak is at $m/z=121$ [$\text{C}_8\text{H}_{11}\text{N}$], and the tenth peak is at $m/z=107$ [$\text{C}_7\text{H}_9\text{N}$], the eleventh at $m/z=93$ [$\text{C}_6\text{H}_7\text{N}$], the twelfth at $m/z=69$ [C_5H_8], which is the peak of the baseline, and the thirteenth at $m/z=56$ [C_4H_8], and that the peak of the baseline proves the validity of the compound. As for the rest of the peaks, they prove the structural shape of the compound, and Scheme (1) shows **that**.

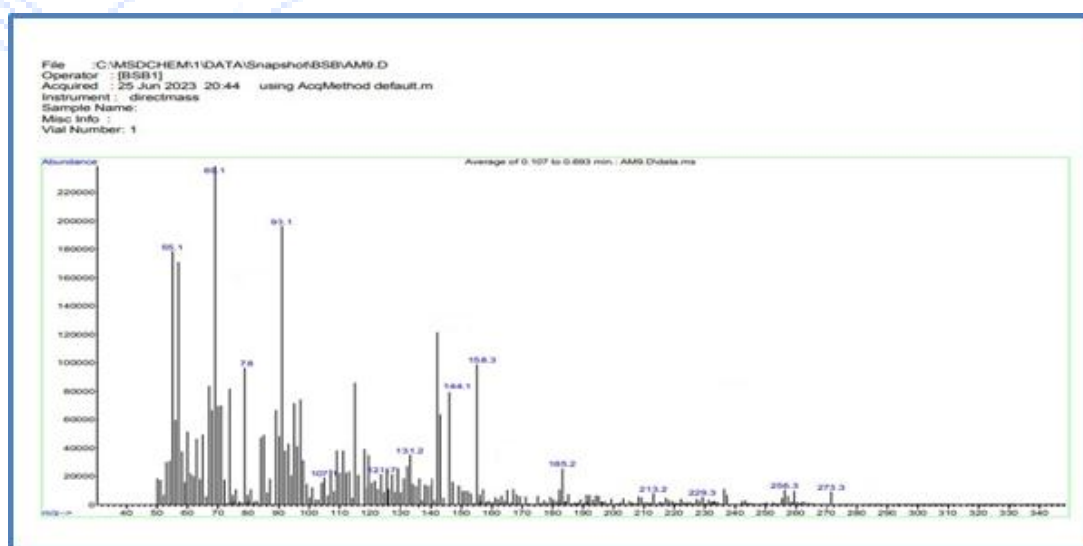
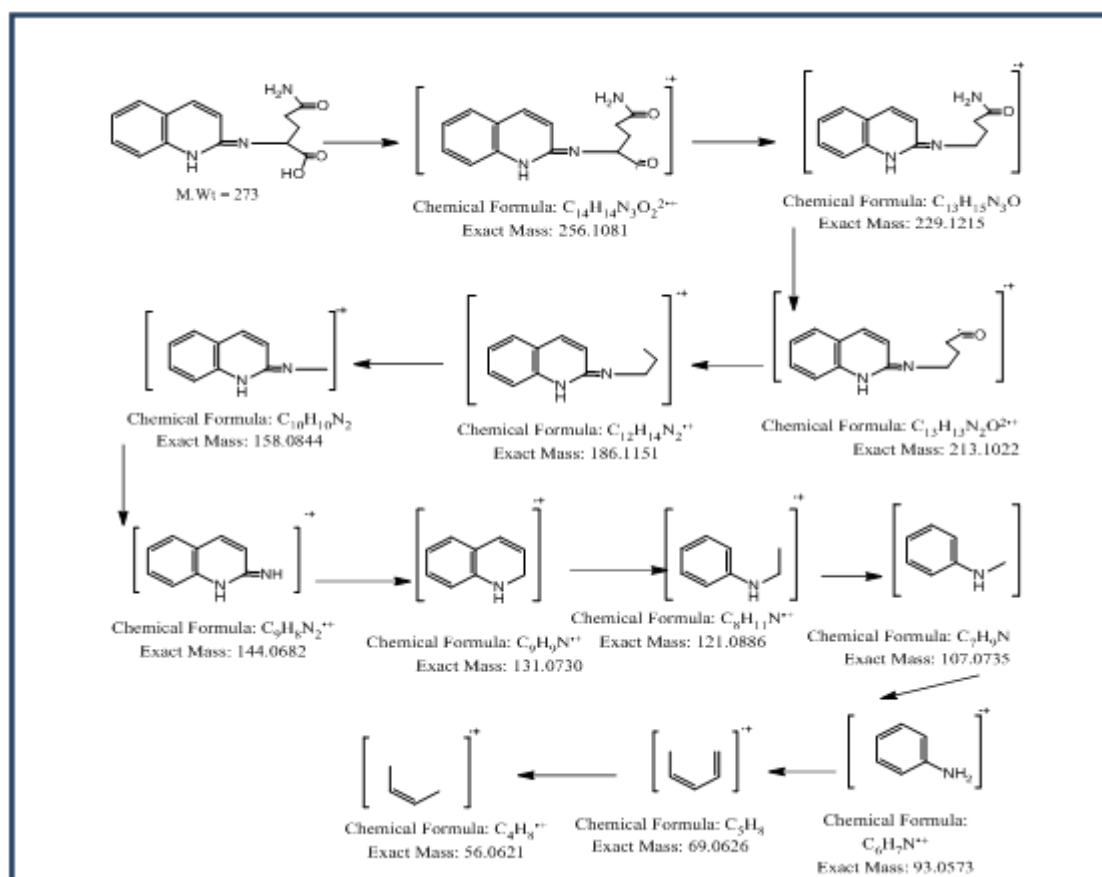


Figure (8) Mass spectrum of the compound [KB8]



Scheme (1): showing the fissions of the compound [KB8]

The integration of the results of the FT-IR spectrum, NMR spectrum, and mass spectrum gives clear evidence of the correctness of the assigned structure of the compound [KB8].

Scanning electron microscopy (SEM) analysis of the prepared compounds

The technique (SEM) is used to take an image of the surfaces of materials, as it is a focused beam of high-energy electrons to generate a variety of signals on the surface of solid samples, where the different signals emanating from the sample reveal information about the sample, including the external shape and crystal structure, whether it is Nanomaterials or not, and a two-dimensional image is created that displays the differences in these properties. Conventional areas whose width ranges from about 1cm to 5 μ m can be imaged in scanning mode. (and resolution potential from 50 to 100 nm, magnification ranges from 20X to about 30,000X) is also capable of performing analyzes of the locations of selected points on the sample, this approach is particularly important for SEM and crystal structure (29,28).

And the SEM analysis of the compound [KB8] shown in Figure (9) showed that (500nm) was used for the cross-sectional area and the magnification power (HV: 70.0KV), and the radii were shown in the Gaussian Fit curve in Graph (1), where the peak was for the radii The compound particles (77.01 nm) are among the nano-assemblies that consist of nano-particles superimposed with each other.

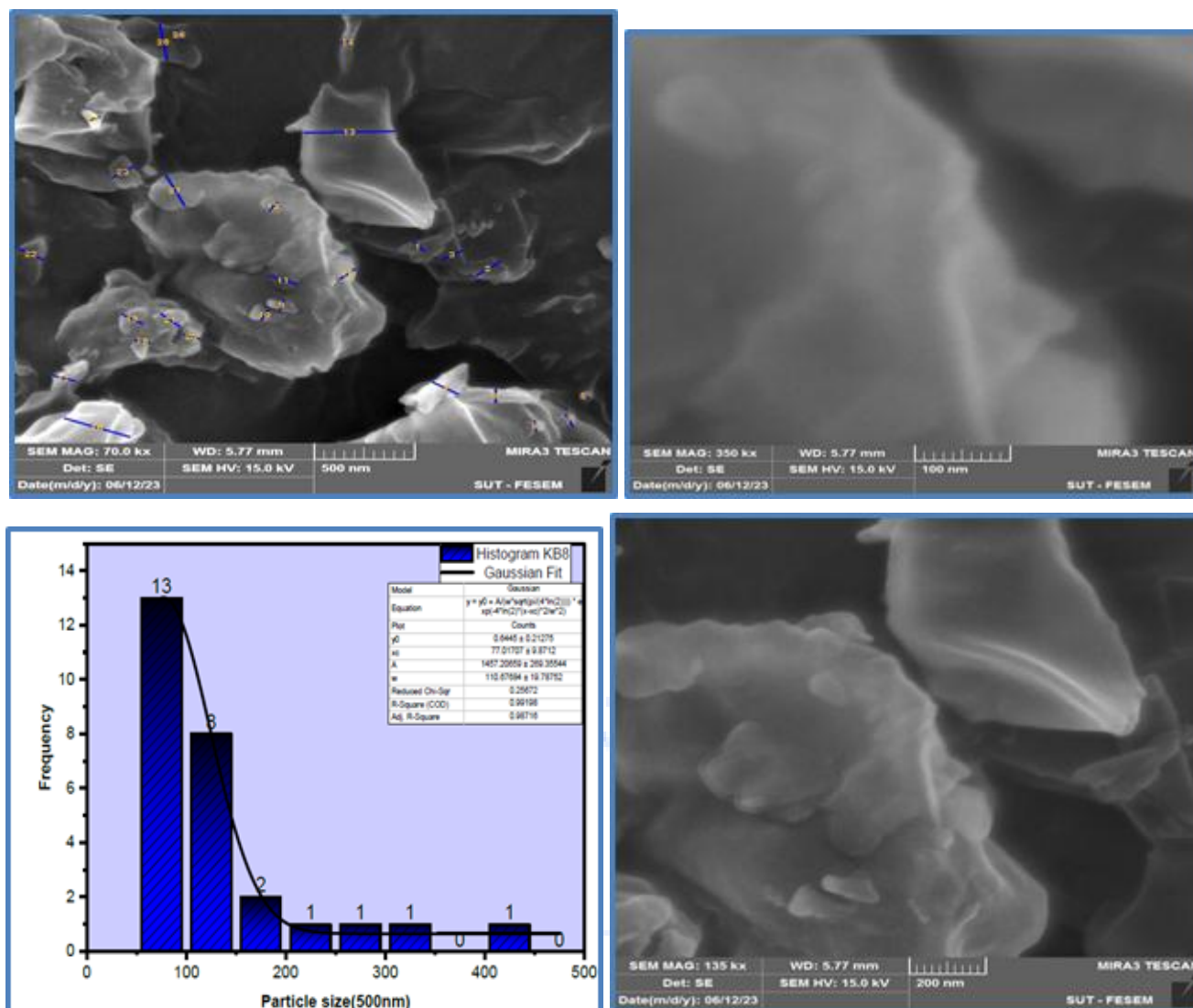


Figure (9) SEM image of compound [KB8] at 500nm

The SEM analysis of the compound [KB11] shown in Figure (10) showed that (500nm) was used for the cross-sectional area and the magnification force was (HV: 70.00KX), and the radii shown in the Gaussian Fit curve were in the graph (4-3), where the peak was The radii of the compound particles are (99.94nm), and these are among the nanoclusters that consist of nanoparticles overlapping with each other.

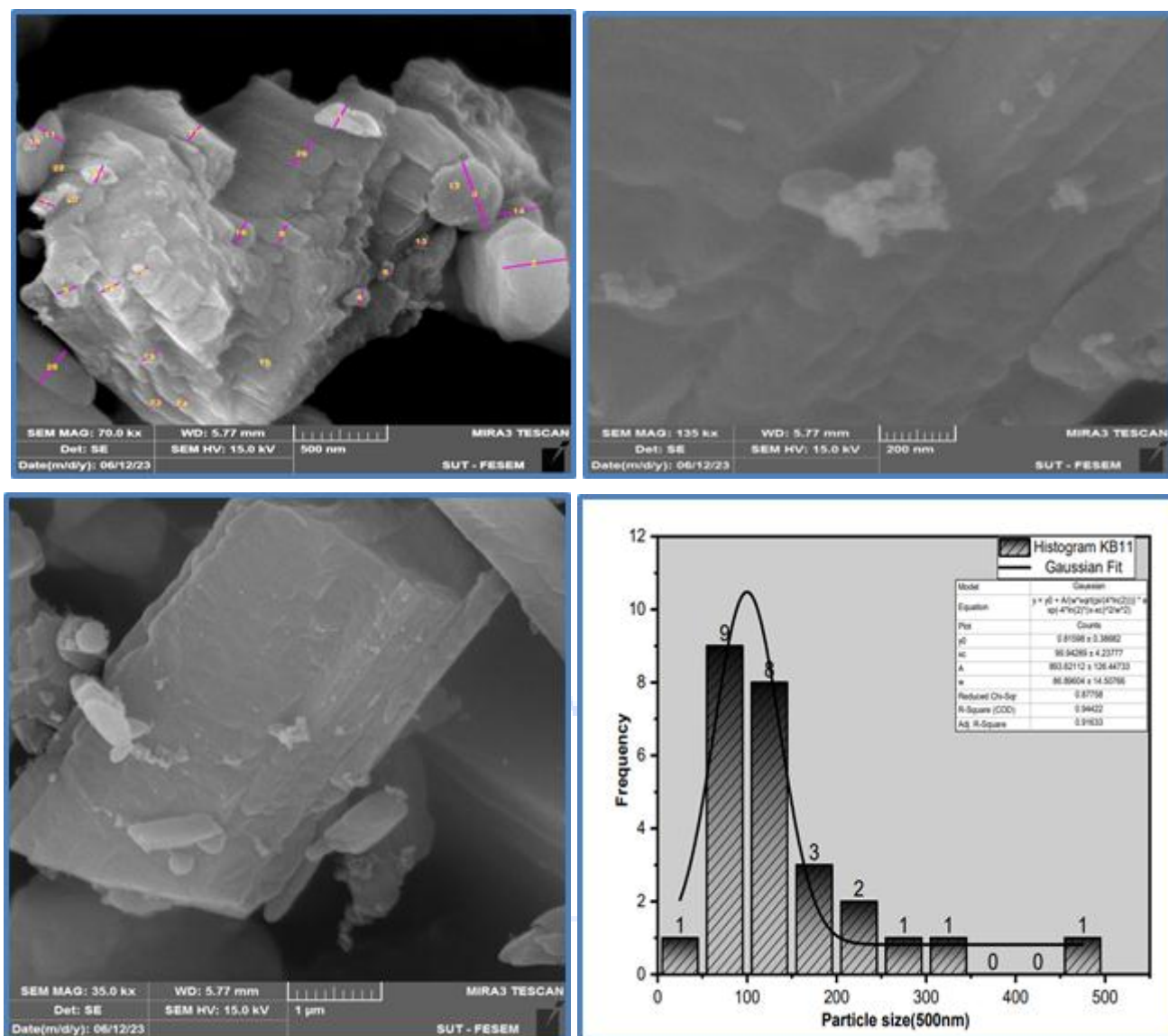


Figure (10) SEM image of compound [KB11] at 500nm

Biological study

The results of investigating biological effectiveness showed that the solutions (KB7, KB11) were effective against both types of the selected bacterial species(30), and the solutions (KB7, KB9, KB11).

The results showed that the lowest effective concentration was against the selected bacterial species(31). The concentration was (A) and in diameters Varied inhibition compared to the concentrated solution (Figure 11). As a comparison with the antibiotic Ampicillin, the results showed the ineffectiveness of this antibiotic and the resistance of bacteria to it compared to the solutions KB7 and KB11, which gave effectiveness(32).

In general, the diameter of the microbial inhibition zones ranged from 18 mm to 22 mm around the holes loaded with solutions, Table No. (3). Solutions that did not give effectiveness were indicated by the symbol n.a, meaning there was no effectiveness.

Table No. (3) The results of the biological activity test for the selected compounds against the bacterial species *Proteus* and *S. faecalis*, measured in millimeters around the agar hole loaded with chemical compounds. The number 0 represents the absence of effectiveness for the secondary concentrations.

<i>Proteus</i>			<i>S. faecalis</i>			
C	B	A	C	B	A	
n.a	n.a	n.a	n.a	n.a	n.a	KB10
0	0	18	0	0	21	KB7
0	0	22	0	0	18	KB11
n.a	n.a	n.a	n.a	n.a	n.a	KB8
n.a	n.a	n.a	n.a	n.a	n.a	KB9

<i>Proteus</i>			<i>S. faecalis</i>			
C	B	A	C	B	A	
0	0	18	0	0	21	KB7
0	0	22	0	0	18	KB11

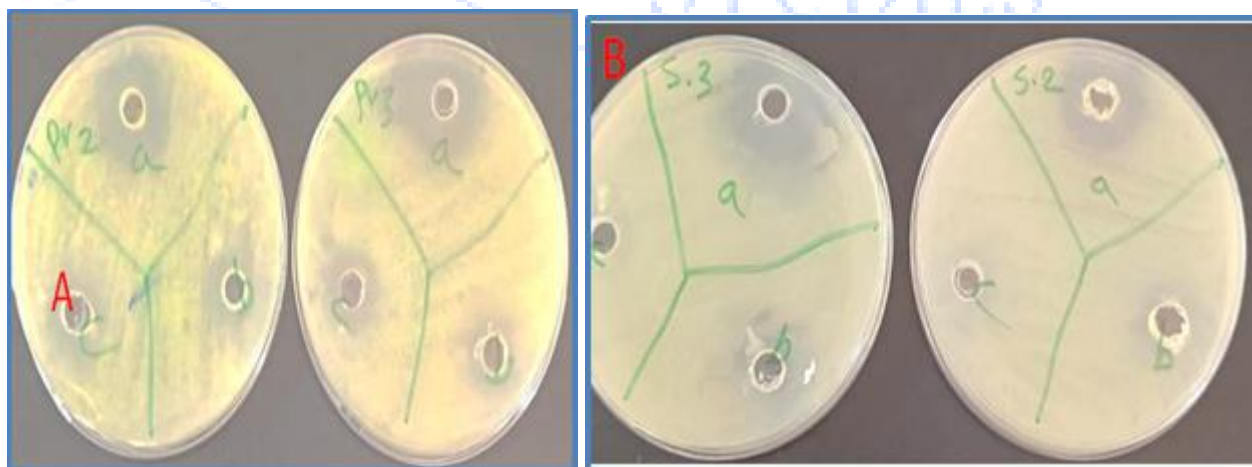


Figure (11) shows the results of culturing bacteria. A is the effect of solutions on Gram-negative *Proteus* bacteria. B is the effect of solutions on Gram-positive *S. faecalis* bacteria. The pits represent places where chemical solutions are loaded, and around them a transparent halo represents an inhibition zone for bacteria.

Thermal analysis study:

The thermal analysis of some prepared compounds was studied using the thermogravimetric decomposition curve (TGA). Information can be obtained from the thermogravimetric curve related to

thermal stability, reaction initiation, and chemical composition of the model, in addition to the thermal stability of the products.

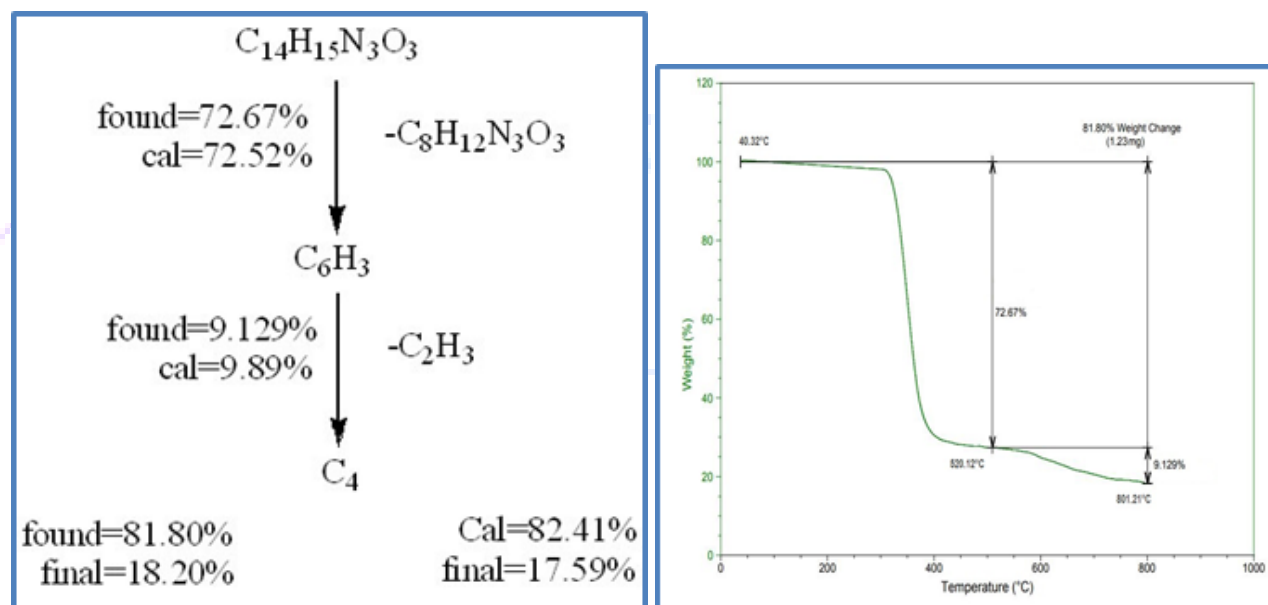
The stages of gravimetric decomposition that the compound goes through (33), as:

Ti = the temperature at which decomposition begins in one step.

Tf = the temperature at which decomposition ends in one step.

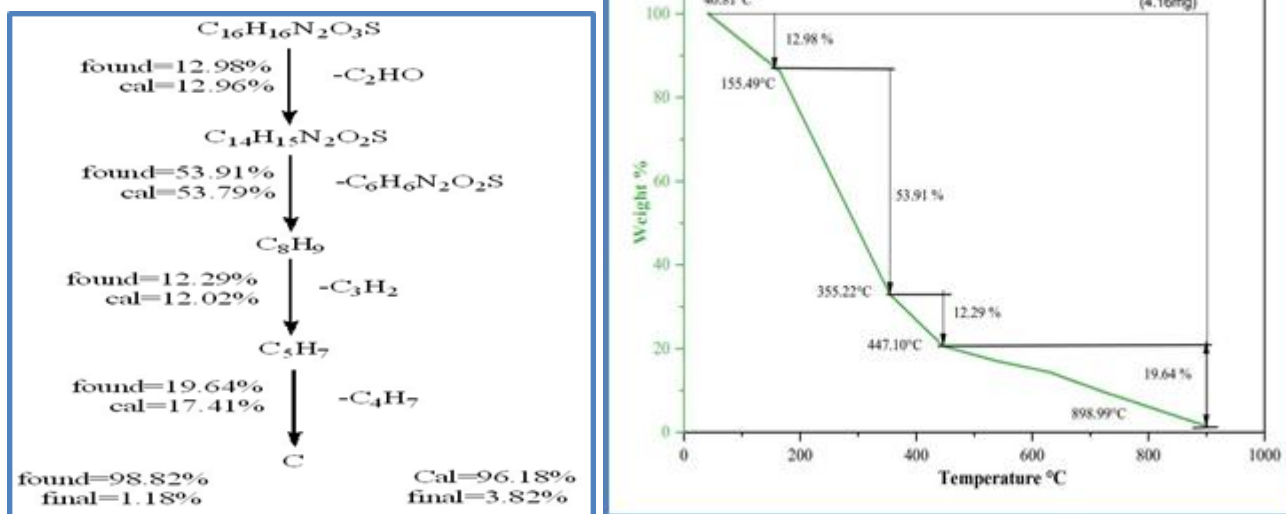
Tmax = maximum temperature for weight loss.

The compound [KB8] showed, using the thermogravimetric decomposition technique, that it decomposes in two stages. The curve shows the disintegration and the critical temperature at which the compound has the maximum transformation (maximum weight loss), and the practical and theoretical percentage lost from each stage is indicated by the mechanics. It is noted from the curve that the first The gravimetric decomposition begins at 200 degrees and ends at 202 degrees, which indicates the stability of the compound before these two temperatures. It also turns out that the total practical weight lost is (81.80)% and the remaining % is (18.20), and theoretically the total lost weight is (82.41) and the remaining is % (17.59). The remainder is (C4) according to the proposed mechanism for the gravimetric decomposition of the compound, as shown in Scheme (2).



Scheme (2) stages of thermogravimetric decomposition of a compound [KB8]

The compound [KB11] showed by the gravimetric pyrolysis technique that it decomposes in four stages, where the curve shows the disintegration and the critical temperature at which the maximum transformation of the compound (maximum weight loss) and the practical and theoretical percentage lost from each stage are indicated by the mechanics, as it is noted through the curve that The first gravimetric decomposition starts at a temperature of 190 and ends at a temperature of 192, which indicates the stability of the compound before these two degrees. It also turns out that the practical total lost weight is (98.82) % and the remaining % is (1.18), and theoretically the total lost weight is (96.18) and the remaining % is (3.82). And that the residue is (C) according to the proposed mechanism of gravimetric decomposition of the compound and as shown in diagram (4).



Scheme (4) stages of thermogravimetric decomposition of a compound [KB11]

4. Conclusions:

Physical and spectroscopic measurements confirmed the accuracy and validity of the prepared compounds. Therefore, the methods used in preparation were good, successful and low cost. Through SEM analysis, the surface of the prepared composites appeared to be rock layers interspersed with deep trenches.

Reference

- Hussain, Maitham Y., Bassam A. Hassan, and Zaman K. Hanan. "Synthesis and Characterization of a new Schiff bases (3Z, 3Z)-3, 3'-((oxybis (4, 1-phenylene)) bis (azanylylidene)) bis (indolin-2-one)." *Turkish Journal of Computer and Mathematics Education (TURCOMAT)* 12.14 (2021): 3341-3351.
- Troschke, Erik, Martin Oschatz, and Ivan K. Ilic. "Schiff-bases for sustainable battery and supercapacitor electrodes." *Exploration*. Vol. 1. No. 3. 2021.
- Subasi, Nuriye Tuna. "Overview of Schiff Bases." *Schiff Base in Organic, Inorganic and Physical Chemistry*. IntechOpen, 2022.
- Mazzoni, Rita, Fabrizio Roncaglia, and Luca Rigamonti. "When the metal makes the difference: Template syntheses of tridentate and tetradentate salen-type schiff base ligands and related complexes." *Crystals* 11.5 (2021): 483.
- Arulmurugan, S., Helen P. Kavitha, and B. R. Venkatraman. "Biological activities of Schiff base and its complexes: a review." *Rasayan J Chem* 3.3 (2010): 385-410.
- Saleh, Ahmed, and Mohanad Y. Saleh. "Synthesis of heterocyclic compounds by cyclization of Schiff bases prepared from capric acid hydrazide and study of biological activity." *Egyptian Journal of Chemistry* 65.12 (2022): 783-792.
- Dalia, S. Afrin, et al. "A short review on chemistry of schiff base metal complexes and their catalytic application." *Int. J. Chem. Stud* 6 (2018): 2859-2866.
- Raczk, Edyta, et al. "Different Schiff bases—Structure, importance and classification." *Molecules* 27.3 (2022): 787.

9. Das, Aparna, and Bimal Krishna Banik. "Dipole moment in medicinal research: green and sustainable approach." *Green Approaches in Medicinal Chemistry for Sustainable Drug Design*. Elsevier, 2020. 921-964.
10. Harreus, A. L., et al. "2-Pyrrolidone." (2011): 1-7.
11. Nechaeva, Anna, et al. "Synthesis of Amphiphilic Copolymers of N-Vinyl-2-pyrrolidone and Allyl Glycidyl Ether for Co-Delivery of Doxorubicin and Paclitaxel." *Polymers* 14.9 (2022): 1727.
12. Tanielyan, Setrak K., et al. "Hydrogenation of succinimide to 2-pyrrolidone over solid catalysts." *Topics in Catalysis* 57 (2014): 1582-1587.25
13. Liu, Wendi, et al. "Soybean oil-based thermosets with N-vinyl-2-pyrrolidone as crosslinking agent for hemp fiber composites." *Composites Part A: Applied Science and Manufacturing* 82 (2016): 1-7.
14. Wu, I-Wen, Ja-Liang Lin, and En-Tsung Cheng. "Acute poisoning with the neonicotinoid insecticide imidacloprid in N-methyl pyrrolidone." *Journal of Toxicology: Clinical Toxicology* 39.6 (2001): 617-621.
15. Wu, Tao, et al. "Additively manufacturing high-performance bismaleimide architectures with ultraviolet-assisted direct ink writing." *Materials & Design* 180 (2019): 107947.
16. Bahramia, Homayoon, et al. "Kinetics and mechanism of the autocatalytic dehydration reaction of L- γ -amino-n-butyric acid to 2-pyrrolidone through radical intermediate in moderately concentrated acidic medium."
17. Makarov, Dmitriy M., Gennadiy I. Egorov, and Arkadiy M. Kolker. "Density of water-2-pyrrolidone mixture a new vibrating tube densimeter from (278.15–323.15) K and up to 70 MPa." *Journal of Molecular Liquids* 335 (2021): 116113.
18. Lertsuphotvanit, Nutdanai, et al. "Sublimation/evaporation behaviors of borneol in-situ forming matrix." *Materials Today: Proceedings* (2023).
19. Cui, Yu, et al. "Synthesis and characterization of rare-earth metal complexes supported by a new pentadentate Schiff base and their application in heteroselective polymerization of rac-lactide." *Catalysis Science & Technology* 5.6 (2015): 3302-3312.
20. Al-Labban, Hutham Mahmood Yousif, Hawraa Mohammed Sadiq, and Ahmed Abduljabbar Jaloob Aljanaby. "Synthesis, Characterization and study biological activity of some Schiff bases derivatives from 4-amino antipyrine as a starting material." *Journal of Physics: Conference Series*. Vol. 1294. No. 5. IOP Publishing, 2019.
21. SALEH, Mohammed Jwher; AL-BADRANY, Khalid A. Preparation, Characterization of New 2-Oxo Pyran Derivatives by AL₂O₃-OK Solid Base Catalyst and Biological Activity Evaluation. *Central Asian Journal of Medical and Natural Science*, 2023, 4.4: 222-230.
22. Saleh, J. N., & Khalid, A. (2023). Synthesis, Characterization and Biological Activity Evaluation of Some New Pyrimidine Derivatives by Solid Base Catalyst AL₂O₃-OBa. *Central Asian Journal of Medical and Natural Science*, 4(4), 231-239.
23. Wang, Minmin, et al. "AIE-active Schiff base compounds as fluorescent probe for the highly sensitive and selective detection of Al³⁺ ions." *Journal of Luminescence* 233 (2021): 117911.
24. Majeed, Noor M., Suha Sahab Abd, and Rehab Kadhim Raheem Al Shemary. "Eco-friendly and efficient composition, diagnosis, theoretical, kinetic studies, antibacterial and anticancer activities

- of mixed some metal complexes of tridentate Schiff base ligand." *International Journal of Pharmaceutical Research* 13.1 (2021).
25. Tomer, Nisha, and Rajesh Malhotra. "Schiff base as a fluorescent sensor derived from chromone moiety for the effective detection of Zn (II) ions." *Journal of Molecular Structure* 1252 (2022): 132124.
26. Goel, Apurva, and Rajesh Malhotra. "Efficient detection of Picric acid by pyranone based Schiff base as a chemosensor." *Journal of Molecular Structure* 1249 (2022): 131619.
27. Robert M. Silverstein, Francis X. Webster, David J. Kiemle, spectrometric Identification of Organic compounds, 7th Ed, JohnWiley & Sons, INC, 2005.
28. Kalam, A., Al-Sehemi, A. G., Assiri, M., Du, G., Ahmad, T., Ahmad, I., & Pannipara, M. Modified solvothermal synthesis of cobalt ferrite (CoFe₂O₄) magnetic nanoparticles photocatalysts for degradation of methylene blue with H₂O₂/visible light. *Results in Physics*, (2018), 8: 1046-1053.
29. Zhou, W., Apkarian, R., Wang, Z. L., & Joy, D. Fundamentals of scanning electron microscopy (SEM). In: *Scanning microscopy for nanotechnology*. Springer, New York, NY, (2006). p. 1-40.
30. AL-JOUBOURY, Wissam Mohammed; AL-BADRANY, Khalid Abdulaziz; ASLI, Nabeel Jamal. N-alkylation of substituted 2-amino benzothiazoles by 1, 4-bis (bromo methyl) benzene on mixed oxides at room temperature and study their biological activity. In: *AIP Conference Proceedings*. AIP Publishing, 2022.
31. MOHAMED, Shifaa A.; AL-BADRANY, Khalid A.; HUSEEN, Maha S. PREPARATION AND STUDY OF BIOLOGICAL ACTIVITY OF PYRIMIDINE COMPOUNDS DERIVED FROM 2-ACETYL PYRIDINE. *Vegueta. Anuario de la Facultad de Geografía e Historia*, 2022, 22: 8.
32. MOHAMED, Shifaa Ayoob; HUSSEIN, Maha Saleh; AL-BADRANY, Khalid A. Synthesis and characterization of pyrazolines and oxazapine derivatives using chalcones as precursor and evaluation of their biological activity. *Samarra Journal of Pure and Applied Science*, 2022, 4.4.
33. Arshad, M., Ur-Rehman, S. A. E. E. D., Qureshi, A. H., Masud, K., Arif, M., Saeed, A., & Ahmed, R. Thermal Decomposition of Metal Complexes of Type MLX₂ (M= Co(II), Cu(II), Zn(II), and Cd(II); L= DIE; X= NO₃⁻) by TG-DTA-DTG Techniques in Air Atmosphere. *Turkish Journal of Chemistry*, (2008), 32.5: 593-604